J. Math. Biol. (2009) 59:535–561
DOI 10.1007/s00285-008-0239-2

Mathematical Biology

An SEIQR model for childhood diseases

David J. Gerberry · Fabio A. Milner

Received: 26 October 2007 / Revised: 29 October 2008 / Published online: 10 December 2008

Abstract It has been shown that the inclusion of an isolated class in the classical SIR model for childhood diseases can be responsible for self-sustained oscillations. Hence, the recurrent outbreaks of such diseases can be caused by autonomous, deterministic factors. We extend the model to include a latent class (i.e. individuals who are infected with the disease, but are not yet able to pass the disease to others) and study the resulting dynamics. The existence of Hopf bifurcations is shown for the model, as well as a homoclinic bifurcation for a perturbation to the model. For historical data on scarlet fever in England, our model agrees with the epidemiological data much more closely than the model without the latent class. For other childhood diseases, our model suggests that isolation is unlikely to be a major factor in sustained oscillations.

Keywords Childhood disease · SEIQR model · Recurrent outbreaks · Bifurcation analysis · Unfolding analysis

Mathematics Subject Classification (2000) 92B05 · 34C23 · 34D10 · 37C29 · 37G15

D. J. Gerberry (✉)
Department of Mathematics, Purdue University,
West Lafayette, IN 47907-2067, USA
e-mail: gerberry@math.purdue.edu

F. A. Milner
Department of Mathematics, Arizona State University,
Tempe, AZ 85287-1804, USA
e-mail: milner@math.asu.edu

1 Introduction

The interest in modeling the dynamics of infectious diseases dates back a very long time, to the pioneering work of Daniel Bernoulli's disease statistics from 1760 on smallpox data [3].

Childhood diseases have several attributes which make them well suited for modeling. They have very short incubation and infectious periods and usually confer lifelong immunity. Also, many childhood diseases are mild enough that they do not alter the natural mortality rate. In this case, the underlying demography of the population can be completely disregarded in the model [6,10,12].

Very frequently models for childhood diseases consist of systems of ordinary differential equations that describe the evolution of the various epidemic classes in the model,

- *susceptibles*: individuals who have never been exposed to the disease agent (usually, a virus);
- *exposed*: asymptomatic individuals who have been in contact with the disease agent;
- *infectious*: individuals who can transmit the disease to others;
- *quarantined*: infectious individuals who are isolated from further contacts during some period of time, usually the length of the infectious period;
- *recovered*: individuals who have ceased being infectious and have acquired immunity to the disease (i.e. they cannot become infected from contact with others nor transmit infection to others).

In any epidemic model it is necessary to have the susceptible and infectious classes; other classes may or may not exist for a particular disease and may or may not be considered in models depending on the objectives of the particular modeling effort.

Feng and Thieme [8] studied an SIQR model for childhood diseases and proved the existence of a Hopf bifurcation that leads to the conclusion that the recurrent outbreaks observed in real life may be due to the usual response of isolating infected children at home (quarantine). In that article, the authors also used historical data for scarlet fever in the United Kingdom to match the model they studied with real life data. The agreement between the real life isolation period and the ones required in the model in order to generate periodic solutions was not very good, possibly because of the lack of an exposed class in the model.

Wu and Feng [17] considered an SIQR model of childhood diseases. A center manifold reduction at a bifurcation point showed the bifurcation to be codimension greater than two. A three-parameter unfolding of the normal form was studied and the perturbed system was shown to have a homoclinic bifurcation.

In the present paper we extend the work of Feng et al. [8,17] from an SIQR model to an SEIQR model and find similar richness in the dynamics. For scarlet fever, we also match incubation and isolation periods in the model to those in real life, obtaining a very satisfactory coincidence.

The structure of our paper is as follows: in the next section we describe the model we analyze, and in Sect. 3 we compute the basic reproduction number and the endemic equilibrium. In Sect. 4 we prove the existence of two Hopf bifurcations and give an

estimate for the periods of the periodic solutions near them. In Sect. 5 we study the behavior of the system near the intersection of the two bifurcation curves, and in Sect. 6 we show the existence of a homoclinic bifurcation for a perturbed system. Finally, in Sect. 7, we fit the model to historical data for childhood diseases in England and Wales from 1897 to 1978.

2 The model

We propose the following model for childhood disease:

$$\begin{aligned}
\frac{d}{dt}S &= \Lambda - \mu S - \sigma S\frac{I}{A},\\
\frac{d}{dt}E &= -(\mu+\gamma_1)E + \sigma S\frac{I}{A},\\
\frac{d}{dt}I &= -(\mu+\gamma_2)I + \gamma_1 E,\\
\frac{d}{dt}Q &= -(\mu+\xi)Q + \gamma_2 I,\\
\frac{d}{dt}R &= -\mu R + \xi Q.
\end{aligned} \tag{1}$$

The population is divided into five classes. The classes are: S, individuals susceptible to the disease; E, individuals who are latently infected (i.e. exposed); I, infectious individuals; Q, isolated or quarantined individuals; and R, individuals that have recovered and are immune to the disease. We let $N = S + E + I + Q + R$ denote the total population and we let $A = S + E + I + R$ denote the active population (i.e. those not isolated). Λ is the rate at which individuals are born into the population; each newborn is assumed to be susceptible. μ denotes the natural death rate; our model assumes no disease-induced death. σ is the per capita infection rate of an average susceptible provided that everyone else is infected. γ_1, γ_2 and ξ are the rates at which individuals leave the exposed, infectious and isolated classes, respectively. Hence, $1/\gamma_1$, $1/\gamma_2$ and $1/\xi$ give the average length of the latent, infectious and isolation periods, respectively. $1/\mu$ is the average life expectancy. I/A gives the probability that a given contact is with an infectious individual. All of the model parameters are positive constants. The model is an extension of the one proposed in [8] which did not include the latent period.

An implicit assumption of our model is that the per capita contact rate is independent of the total population size. Evidence suggests that this assumption is realistic provided that the active population does not become too small [9,18].

In order to facilitate the analysis of the system, we attempt to reduce its dimension and reduce the number of parameters. Recalling that $N = S + E + I + Q + R$ is the total population size, we note that

$$\frac{d}{dt}N = \Lambda - \mu N.$$

Hence, $N(t) \to \Lambda/\mu$ as $t \to \infty$. By assuming that the total population has reached its limiting value (i.e. $N(t) \equiv \Lambda/\mu$), we are able to eliminate S from our system. Using that $S = A - E - I - R$ the resulting system is

$$\begin{aligned}
\frac{d}{dt}E &= -(\mu+\gamma_1)E + \sigma\left(1 - \frac{E+I+R}{A}\right)I,\\
\frac{d}{dt}I &= -(\mu+\gamma_2)I + \gamma_1 E,\\
\frac{d}{dt}Q &= -(\mu+\xi)Q + \gamma_2 I,\\
\frac{d}{dt}R &= -\mu R + \xi Q.
\end{aligned} \tag{2}$$

Next, we scale time so that $\sigma = 1$ by introducing a new dimensionless time $\tau = \sigma t$. Lastly, to get a system with linear and quadratic relationships only, we let

$$s = \frac{S}{A}, \quad z = \frac{E}{A}, \quad p = \frac{I}{A}, \quad q = \frac{Q}{A}, \quad r = \frac{R}{A}.$$

The reduced system is then

$$\begin{aligned}
\frac{dz}{d\tau} &= z[-\nu - \theta_1 + \theta_2 p - (\nu+\zeta)q] + p(1-p-r-z),\\
\frac{dp}{d\tau} &= p[-\nu - \theta_2 + \theta_2 p - (\nu+\zeta)q] + \theta_1 z,\\
\frac{dq}{d\tau} &= (1+q)[\theta_2 p - (\nu+\zeta)q],\\
\frac{dr}{d\tau} &= r[-\nu + \theta_2 p - (\nu+\zeta)q] + \zeta q,
\end{aligned} \tag{3}$$

where

$$\nu = \frac{\mu}{\sigma}, \quad \theta_1 = \frac{\gamma_1}{\sigma}, \quad \theta_2 = \frac{\gamma_2}{\sigma}, \quad \zeta = \frac{\xi}{\sigma}. \tag{4}$$

The biologically feasible region for our system is $B = \{(p, z, q, r) : z, p, q, r \geq 0 \text{ and } z + p + r \leq 1\}$. Note that q can be greater than 1, because $q = Q/A$ and the quarantined class is not contained in the active population. It can be shown that B is invariant for (3).

3 Basic reproductive number and the endemic equilibrium

The *basic reproductive number,* $\mathcal{R}_0$, gives the total number of secondary infections that an average infectious individual will induce given that the rest of the population is susceptible. To calculate this, note that the length of an average infection is $\frac{1}{\gamma_2+\mu}$, and recall that σ is the per capita rate of transmitting the disease. Lastly, the probability

of an exposed individual becoming infectious before dying is $\frac{\gamma_1}{\gamma_1+\mu}$. Thus, we can propose the following expression for the reproductive number:

$$\mathcal{R}_0 = \frac{\gamma_1}{\gamma_1+\mu}\frac{\sigma}{\gamma_2+\mu} = \frac{\theta_1}{(\theta_1+\nu)(\theta_2+\nu)}. \tag{5}$$

Due to the structure of our epidemiological system, it is known that the mathematics will confirm this intuitive quantity [4].

For all possible parameter values, the system possesses a disease-free equilibrium (DFE), $(z^*, p^*, q^*, r^*) = (0, 0, 0, 0)$. To seek endemic equilibria we look for (z^*, p^*, q^*, r^*) such that all of the right hand sides of (3) are 0. The resulting equilibrium is

$$z^* = \frac{\nu(\nu+\theta_2)(\nu+\zeta)\kappa}{\theta_1}, \quad p^* = \nu(\nu+\zeta)\kappa, \quad q^* = \theta_2\nu\kappa, \quad r^* = \theta_2\zeta\kappa, \tag{6}$$

where

$$\kappa = \frac{\theta_1 - (\nu+\theta_1)(\nu+\theta_2)}{\nu(\nu+\theta_1+\theta_2)(\nu+\zeta)+\zeta\theta_1\theta_2}. \tag{7}$$

In order to have a positive equilibrium, we need $\kappa > 0$. However, using (7) and (5) we find this condition is equivalent to $\mathcal{R}_0 > 1$.

Since $\mathcal{R}_0$ gives the average number of new infections that a single infectious individual will induce, one would expect from a biological perspective that the disease should die out in the situation where $\mathcal{R}_0 < 1$. This intuition is confirmed via analysis. To see this, we can linearize our system of ODE's (3) around the DFE. Let $X = (z, p, q, r)^T$, and rewrite (3) as $X' = F(X)$. The Jacobian of F at the DFE, $X^* = (0, 0, 0, 0)^T$, is

$$DF(X^*) = \begin{bmatrix} -\nu-\theta_1 & 1 & 0 & 0 \\ \theta_1 & -\nu-\theta_2 & 0 & 0 \\ 0 & \theta_2 & -\nu-\zeta & 0 \\ 0 & 0 & \zeta & -\nu \end{bmatrix},$$

and has real eigenvalues $-\nu$, $-\nu-\zeta$, $-\nu-\frac{1}{2}(\theta_1+\theta_2) \pm \frac{1}{2}\sqrt{(\theta_1-\theta_2)^2+4\theta_1}$. After some manipulation, one finds that all eigenvalues are negative when $\mathcal{R}_0 < 1$. Thus, in this case the DFE is locally asymptotically stable. In fact, one can show that when $\mathcal{R}_0 < 1$ the DFE is *globally* asymptotically stable. That is, for any feasible initial data (z_0, p_0, q_0, r_0) we have that $(z, p, q, r) \to (0, 0, 0, 0)$ as $t \to \infty$. The proof of this follows that of [7] which uses the approach to persistence of Thieme [14,15] and we do not include it here. If $\mathcal{R}_0 > 1$, the Jacobian has one positive eigenvalue and the DFE loses its stability.

We summarize these findings in the following Proposition:

Proposition 1 *For the model described by (3), the following holds*:

(i) *The biologically feasible region* $B = \{(p, z, q, r) : z, p, q, r \geq 0$ *and* $z + p + r \leq 1\}$ *is invariant under the dynamics of our model.*
(ii) *If* $\mathcal{R}_0 < 1$, *system (3) possesses only the DFE.*
(iii) *If* $\mathcal{R}_0 < 1$, *the DFE is globally asymptotically stable.*
(iv) *If* $\mathcal{R}_0 > 1$, *the DFE is not stable.*
(v) *If* $\mathcal{R}_0 > 1$, *there is a uniquely determined positive equilibrium given by (6).*

4 Hopf bifurcation of the endemic equilibrium and sustained oscillations

We consider the linearization of our system about the endemic equilibrium in order to study the emergence of sustained oscillations. Again, we let $X = (z, p, q, r)^T$, and rewrite (3) as $X' = F(X)$. We will denote the Jacobian of F at the endemic equilibrium, $X^* = (z^*, p^*, q^*, r^*)^T$, as $DF(X^*)$. Explicit calculation gives that the characteristic polynomial has the form

$$|wI - DF(X^*)| = w^4 + aw^3 + bw^2 + cw + d,$$

where each of a, b, c, and d is of the form

$$\frac{P_U(\theta_1, \theta_2, \zeta, \nu)}{Q(\theta_1, \theta_2, \zeta, \nu)},$$

for some polynomial $P_U(\theta_1, \theta_2, \zeta, \nu)$ where $U \in \{a, b, c, d\}$ and $Q(\theta_1, \theta_2, \zeta, \nu) = \nu^3 + (\zeta + \theta_1 + \theta_2)\nu^2 + \zeta(\theta_1 + \theta_2)\nu + \theta_1\theta_2\zeta$. Recalling that $\theta_1, \theta_2, \zeta$, and ν are all positive, we have that a, b, c, and d are analytic functions of ν.

Taking a step back, we recall that μ is the natural death rate. Accordingly, $1/\mu$ is the average life expectancy which is on the order of decades. In comparison, $1/\gamma_1$, $1/\gamma_2$ and $1/\xi$ are the average lengths of the latent, infectious and isolated periods, respectively. Each of these is on the order of days. Thus, μ is much smaller than any of γ_1, γ_2, or ξ and thus by (4), $\nu \ll \theta_1, \theta_2, \zeta$. Using this fact and the expression for the basic reproductive number (5), we see that $\mathcal{R}_0 \approx \frac{1}{\theta_2}$. As it is known that the DFE is globally asymptotically stable when $\mathcal{R}_0 < 1$, we assume that $\mathcal{R}_0 > 1$ while examining the possible Hopf bifurcation of the endemic equilibrium. Thus, we have that $\nu \ll \theta_2 \approx 1/\mathcal{R}_0 < 1$. Further, we can assert that $\theta_1, \theta_2, \zeta \sim O(\frac{1}{\mathcal{R}_0})$ since each of the corresponding original time periods were on the order of days. With this in mind, we consider the series expansions of a, b, c, and d near $\nu = 0$ and get

$$\begin{aligned}
a &= \theta_1 + \theta_2 + \zeta + \frac{3\theta_2 + 1}{\theta_2}\nu + O(\nu^2),\\
b &= \zeta\,(\theta_1 + \theta_2) + \frac{2\theta_2\zeta + \zeta + \theta_1\theta_2 + \theta_2 + {\theta_2}^2 + \theta_1}{\theta_2}\nu + O(\nu^2),\\
c &= \frac{\theta_2\zeta + \theta_1{\theta_2}^3 + \theta_1\theta_2 - 2\theta_1{\theta_2}^2 + \theta_1\zeta}{\theta_2}\nu + O(\nu^2),\\
d &= \theta_1\zeta\,(1 - \theta_2)\,\nu + O(\nu^2).
\end{aligned} \tag{8}$$

In the limiting case, $\nu = 0$, the characteristic equation is

$$w^4 + (\theta_1 + \theta_2 + \zeta)w^3 + \zeta(\theta_1 + \theta_2)w^2,$$

with simple roots at $-(\theta_1 + \theta_2)$ and $-\zeta$ and a double root at 0.

Kato [11] (Ch. 2 §1.2) discusses analytic perturbation theory for linear operators. Considering (3) as an analytic perturbation in ν about $\nu = 0$, it follows that there are four continuous branches $w_\triangledown$, $w_\diamondsuit$, w_-, and w_+ of roots of the characteristic equation defined for small $\nu > 0$ that satisfy $w_\triangledown(0) = -(\theta_1 + \theta_2)$, $w_\diamondsuit(0) = -\zeta$, $w_\pm(0) = 0$. From [11], we also know that

$$w_\triangledown(\nu) = -(\theta_1 + \theta_2) + \sum_{j=1}^{\infty} w_j \nu^j, \quad w_\diamondsuit(\nu) = -\zeta + \sum_{j=1}^{\infty} w_j \nu^j,$$

and that $w_\pm(\nu)$ can have one of two possible expansions. Either

$$w_\pm(\nu) = \sum_{j=1}^{\infty} w_j \nu^j, \quad \text{or} \quad w_\pm(\nu) = \sum_{j=1}^{\infty} w_j \nu^{j/2}.$$

Substituting the first expansion into the characteristic equation, we get

$$\begin{aligned} 0 = &\left(w_1\nu + O(\nu^2)\right)^4 + a\left(w_1\nu + O(\nu^2)\right)^3 \\ &+ b\left(w_1\nu + O(\nu^2)\right)^2 + c\left(w_1\nu + O(\nu^2)\right) + d. \end{aligned}$$

Recalling the expressions for a, b, c, and d in (8), we see that this simplifies to $(\zeta\theta_1^2\theta_2 - \zeta\theta_1^2\theta_2^2)\nu + O(\nu^2) = 0$. Hence, there are no values of w_j for which this expansion gives roots of the characteristic equation.

Fitting the second possibility into our characteristic equation yields

$$\begin{aligned} 0 = \ &\theta_1\theta_2\zeta\left[w_1^2(\theta_1 + \theta_2) - \theta_1(1 - \theta_2)\right]\nu + w_1\theta_1\Big[(\zeta + \theta_2 + \theta_1)\theta_2 w_1^2 \\ &+ (\theta_2 + \theta_1)2\zeta\theta_2 w_2 + \theta_1\theta_2(1 - \theta_2)^2 + \zeta(\theta_1 + \theta_2)\Big]\nu^{3/2} + O(\nu^2). \end{aligned}$$

Solving for w_1 and w_2, we get

$$w_1 = \pm\sqrt{\frac{\theta_1(\theta_2 - 1)}{\theta_1 + \theta_2}} = \pm\sqrt{\frac{\theta_1(1 - \theta_2)}{\theta_1 + \theta_2}}\,i, \tag{9}$$

(a straightforward calculation using (5) shows that $\theta_2 < 1$ when $\mathcal{R}_0 > 1$) and

$$w_2 = -\theta_1\theta_2^4 + (\theta_1 - \theta_1^2)\theta_2^3 + (\theta_1^2 - \zeta\theta_1 - \zeta)\theta_2^2 - \zeta\theta_1\theta_2 - \theta_1^2\zeta.$$

The four roots of the characteristic equation are thus given by $w_\triangledown(\nu) = -(\theta_1 + \theta_2) + O(\nu)$, $w_\diamondsuit(\nu) = -\zeta + O(\nu)$, and $w_\pm(\nu) = w_1\nu^{1/2} + w_2\nu^{3/2} + O(\nu^2)$. To find a Hopf bifurcation, we are interested in the event that the eigenvalues cross the imaginary axis. Since w_1 is purely imaginary and w_2 is real, this amounts to setting $w_2 = 0$.

Fixing θ_1 and θ_2 and using ζ as a bifurcation parameter, we see that the roots of the characteristic equation cross the imaginary axis near

$$\zeta = \frac{\theta_1\theta_2^2(1-\theta_2)(\theta_1+\theta_2)}{\theta_2^2(\theta_1+1)+\theta_1\theta_2+\theta_1^2}. \tag{10}$$

To check that the crossing is transversal, we note that $\frac{d}{d\zeta}(\text{Re } w_\pm) = [-(\theta_1+1)\theta_2^2 - \theta_1\theta_2 - \theta_1^2] * \nu^{3/2} + O(\nu^2) < 0$ for sufficiently small ν. Hence, nonresonance holds and there is a Hopf bifurcation near (10). Numerical experiments suggest that the Hopf bifurcation is supercritical. We summarize our discussion in the following theorem.

Theorem 1 *There is a function $\zeta_0(\nu)$ defined for small $\nu > 0$,*

$$\zeta_0(\nu) = \frac{\theta_1\theta_2^2(1-\theta_2)(\theta_1+\theta_2)}{\theta_2^2(\theta_1+1)+\theta_1\theta_2+\theta_1^2} + O(\nu^{1/2}), \tag{11}$$

with the following properties:

1. *The endemic equilibrium is locally asymptotically stable if $\zeta > \zeta_0(\nu)$ and unstable if $\zeta < \zeta_0(\nu)$, provided that ζ does not become "too small."*
2. *There is a Hopf bifurcation of periodic solutions at $\zeta = \zeta_0(\nu)$ for small enough $\nu > 0$. In the neighborhood of the Hopf bifurcation, the periods of these solutions are approximately*

$$T = \frac{2\pi\sqrt{\theta_1+\theta_2}}{\sqrt{\nu\theta_1(1-\theta_2)}}.$$

The approximation of periods near the Hopf bifurcation is obtained by recalling that a linear system of ODE's having eigenvalues $\lambda = x \pm iy$, has a period of $2\pi/y$. In our case, the imaginary part of the eigenvalues can be approximated using (9).

Numerical experiments with (3) verify the existence of this Hopf bifurcation but also suggest that a second Hopf bifurcation occurs for values of ζ much smaller than $\zeta_0(\nu)$. To obtain a general location of the second Hopf bifurcation, we consider various values of ν and fix all other parameters. For each ν, the bifurcating value of ζ is estimated numerically. Noticing that the ratio of ν to ζ remained constant, we assume that $\zeta = \eta\nu$ and look for the Hopf bifurcation in the same manner as before.

With this substitution in mind, recall that the characteristic equation of the linearization of our system at the endemic equilibrium is given by (8). In the limiting case, $\nu = 0$, the characteristic equation is now $w^4 + (\theta_1+\theta_2)w^3 = 0$ with roots $w = -(\theta_1+\theta_2)$ and a triple root at $w = 0$. We again appeal to Kato [11] (Ch. 2 §1.2)

for insight into the eigenvalues when ν is near 0. As before, there are four continuous branches w_∇, $w_\diamondsuit$, w_-, and w_+ of roots of the characteristic equation defined for small $\nu > 0$ that satisfy $w_\nabla(0) = -(\theta_1+\theta_2)$, $w_\diamondsuit(0) = 0$, $w_\pm(0) = 0$. From [11], we know that

$$w_\nabla(\nu) = -(\theta_1+\theta_2) + \sum_{j=1}^{\infty} w_j \nu^j,$$

and that $w_\diamondsuit(\nu)$ and $w_\pm(\nu)$ can have one of three possible expansions. The possibilities are

$$\sum_{j=1}^{\infty} w_j \nu^j, \quad \sum_{j=1}^{\infty} w_j \nu^{j/2}, \quad \text{or} \quad \sum_{j=1}^{\infty} w_j \nu^{j/3}.$$

Substituting the first expansion into the characteristic equation, we get

$$\begin{aligned} 0 = &\left(w_1\nu + O(\nu^2)\right)^4 + a\left(w_1\nu + O(\nu^2)\right)^3 \\ &+ b\left(w_1\nu + O(\nu^2)\right)^2 + c\left(w_1\nu + O(\nu^2)\right) + d, \end{aligned}$$

which simplifies to

$$-\eta\theta_1^2\theta_2^2(1-\theta_2)(1+\eta)\left(-\eta+\theta_2-1-w_1(1-\theta_2)\right)\nu^2 + O(\nu^3) = 0.$$

Solving for w_1, yields

$$w_\diamondsuit(\nu) = w_1\nu + O(\nu^2) = \frac{-(\eta+1-\theta_2)}{1-\theta_2}\nu + O(\nu^2).$$

Substituting the second expansion into the characteristic equation, we get

$$\begin{aligned} 0 = &\left(w_1\nu^{1/2} + w_2\nu + O(\nu^{3/2})\right)^4 + a\left(w_1\nu^{1/2} + w_2\nu + O(\nu^{3/2})\right)^3 \\ &+ b\left(w_1\nu^{1/2} + w_2\nu + O(\nu^{3/2})\right)^2 + c\left(w_1\nu^{1/2} + w_2\nu + O(\nu^{3/2})\right) + d, \end{aligned}$$

which simplifies to

$$\begin{aligned} 0 = \ &\eta\theta_1\theta_2^2 w_1\left(\eta(\theta_1+\theta_2)w_1^2 + \theta_1(1-\theta_2)^2(1+\eta)\right)\nu^{3/2} + \theta_1^2\theta_2(1+\eta)(1-\theta_2) \\ &\times\Big[-2\eta\theta_2(1-\theta_2)(\theta_1+\theta_2)^2 w_2 + \eta^2\theta_2^2(\theta_1+\theta_2)^2 + \eta(1-\theta_2)(\theta_2^3\theta_1 - 2\theta_1\theta_2^2\theta_2 \\ &-\theta_2^2 - \theta_1\theta_2 - \theta_1^2) - (1-\theta_2)^2(\theta_1^2+\theta_2^2+\theta_1\theta_2(\theta_2+1))\Big]\nu^2 + O(\nu^{5/2}). \end{aligned}$$

Solving, we find that w_1 can be 0 or $\pm i(1-\theta_1)\sqrt{\frac{\theta_1(1+\eta)}{\eta(\theta_1+\theta_2)}}$. Letting $w_1 = 0$ eliminates the $\nu^{1/2}$ term in our expansion and leads us to the same expansion we found for $w_\diamondsuit(\nu)$. Using the other possibility we find that

$$w_2 = \frac{1}{2\eta}(A\eta^2 + B\eta + C),$$

where

$$\begin{aligned} A &= \frac{\theta_2}{1-\theta_2}, \\ B &= \frac{\theta_1(1-\theta_2)^2}{(\theta_1+\theta_2)^2} - \frac{1}{\theta_2}, \\ C &= \frac{\theta_1(1-\theta_2)^2}{(\theta_1+\theta_2)^2} - \frac{1-\theta_2}{\theta_2}. \end{aligned}$$

To find the Hopf bifurcation, we need the eigenvalues to cross the imaginary axis. As in our first expansion, w_1 is purely imaginary and w_2 is real. Thus, by setting $w_2 = 0$, solving for η, and recalling that $\zeta = \eta\nu$, we find the Hopf bifurcation.

Theorem 2 *There is a function $\zeta_1(\nu)$ defined for small $\nu > 0$,*

$$\zeta_1(\nu) = \frac{\frac{1}{\theta_2} - \frac{\theta_1(1-\theta_2)^2}{(\theta_1+\theta_2)^2} + \sqrt{\left(\frac{\theta_1(1-\theta_2)^2}{(\theta_1+\theta_2)^2} - \frac{1}{\theta_2}\right)^2 - 4\theta_2\left(\frac{\theta_1(1-\theta_2)}{(\theta_1+\theta_2)^2} - \frac{1}{\theta_2}\right)}}{\frac{2\theta_2}{1-\theta_2}}\nu + O(\nu^{3/2}),$$

with the following properties:

1. *The endemic equilibrium is locally asymptotically stable if $\zeta < \zeta_1(\nu)$ and unstable if $\zeta > \zeta_1(\nu)$, provided that ζ does not become "too large."*
2. *There is a Hopf bifurcation of periodic solutions at $\zeta = \zeta_1(\nu)$ for small enough $\nu > 0$.*

An estimate of the periods of such solutions near the Hopf bifurcation can be obtained in the same way as in Theorem 1. We omit the exact expression for clarity of presentation. We also omit the calculation that $\frac{d}{d\zeta}(\text{Re } w_\pm) > 0$ at $\zeta = \zeta_1(\nu)$ which confirms the transversality of this crossing.

With Theorems 1 and 2 established, we have a rich understanding of the behavior of our system, (3), in full parameter space. For each fixed ν, we can plot $\zeta_0(\nu)$ and $\zeta_1(\nu)$ (see Fig. 1). Recall that $\mathcal{R}_0 > 1$ implies that $\theta_2 < 1$. We see that the inclusion of the latent class can lead to the loss of sustained oscillations provided the latent period is long enough (i.e. θ_1 is small enough). Numerical experiments confirm that for parameter values in the region between $\zeta_0(\nu)$ and $\zeta_1(\nu)$ our model exhibits sustained oscillations. The only area of question lies in the intersection of the surfaces that occurs for smaller values of θ_2. We discuss this in detail in the following section.

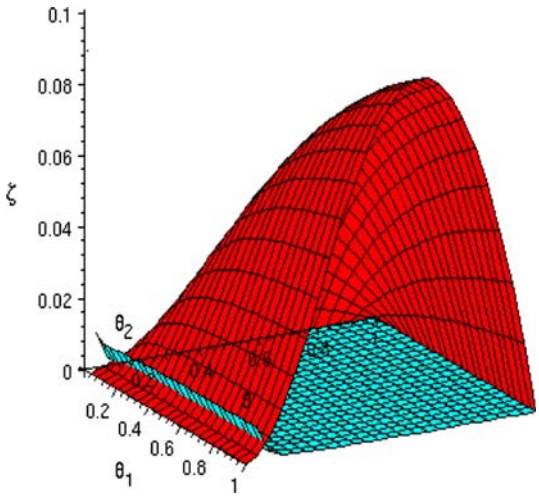

Fig. 1 $\zeta_0(\nu)$, (*dark*), and $\zeta_1(\nu)$, (*light*), for $\nu = 0.00003$

5 Intersection of $\zeta_0(\nu)$ and $\zeta_1(\nu)$

We begin by recalling the assumptions used to find the Hopf bifurcations. The first Hopf bifurcation was derived assuming that the isolation period is on the order of the duration of infection (i.e. $\zeta_0 \sim O(\theta_2) \gg \nu$). The second assumed that the isolation period is on the order of life span (i.e. $\zeta_1 \sim O(\nu)$). Therefore, it is biologically infeasible for both assumptions to be satisfied simultaneously. Regardless, the intersection of the ζ_0 and ζ_1 is still of mathematical interest. Our analysis indicates that Hopf bifurcations occur near both $\zeta_0(\nu)$ and $\zeta_1(\nu)$. With this in mind, the intersection of the two surfaces either indicates extremely complex dynamics or is a consequence of the approximations used in the previous section.

To simplify our discussion, we consider the limiting system as $\theta_1 \to \infty$. Biologically, we recall that θ_1 is the rate at which individuals leave the latent class. Thus, the limiting system is identical to that of [8] which does not include a latent class.

Numerical experiments have shown that this intersection is in fact a product of our approximations and is not indicative of the true behavior of our system (see Fig. 2). This is not surprising since the fact that $\nu \ll \theta_1, \theta_2, \zeta$ was paramount in our ability to use Taylor series expansions in the previous section. Thus, we should expect large errors in our approximations as any of θ_1, θ_2, or ζ become small. However, noticing that Fig. 2 corresponds to $\nu = 0.001$, and that our approximations fail for $\theta_2 \approx 0.27$, it appears to still be the case that $\nu \ll \theta_2$. Recalling (11), the expression for ζ_0 given in Theorem 1, we have that

$$\lim_{\theta_1 \to \infty} \zeta_0(\nu) = \theta_2^2(1 - \theta_2) + O(\nu^{1/2}).$$

Thus we may expect our approximation to fail when $\theta_2^2(1 - \theta_2) \approx O(\nu^{1/2})$. As θ_2 becomes small, this is equivalent to $\theta_2 \approx O(\nu^{1/4})$. To verify that this is indeed the location of observed error in ζ_0, we repeat the numerical experiments to get graphs

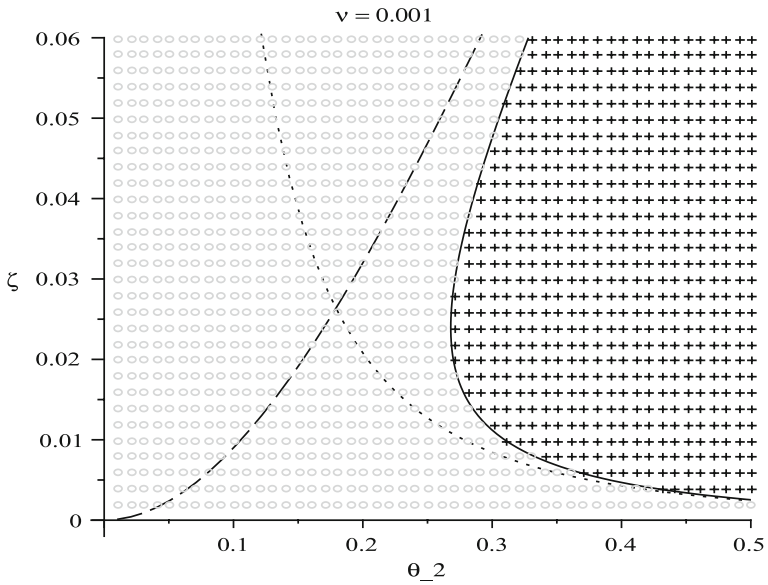

Fig. 2 Intersection of $\zeta_0(\nu)$ (*dashed*), $\zeta_1(\nu)$ (*dotted*), and actual Hopf bifurcation curve (*solid*), for $\nu = 0.001$. *plus symbol* indicates sustained oscillations, *open circle* indicates a stable endemic equilibrium

Table 1 Comparison of the location of observed error and $\nu^{1/4}$ for various values of ν

ν	$\nu^{1/4}$	Obs. error	Obs./$\nu^{1/4}$
0.005	0.26591	0.428	1.61
0.001	0.17783	0.268	1.51
0.0005	0.14953	0.223	1.49
0.0001	0.10000	0.146	1.46
0.00005	0.08409	0.122	1.45
0.00001	0.05623	0.082	1.46
0.000005	0.04729	0.068	1.44

similar to Fig. 2 for various values of ν. Using the minimum value of θ_2 for which sustained oscillations occur as the value for which "observed error" occurs, we can compare the value of "observed error" and $\nu^{1/4}$ for various values of ν. As this ratio remains relatively constant (see Table 1), we believe this to be the correct location for dominant roundoff errors. At this time, a similar understanding of $\zeta_1(\nu)$ has eluded the authors.

6 Homoclinic bifurcation of a "nearby" system

Numerical studies with Doedel's program *Auto* [5] indicate that as ζ moves away from $\zeta_0(\nu)$ or $\zeta_1(\nu)$ that the period of the sustained oscillations increases seemingly slower than linearly. This may affect *Auto's* ability to continue its calculations further away from the bifurcations (see Fig. 3). This leads one to suspect the occurrence of

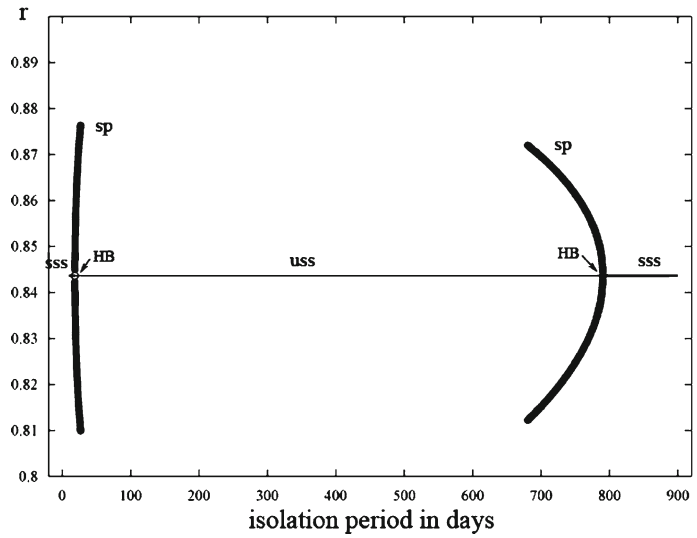

Fig. 3 An Auto plot of the lower and upper amplitudes of the periodic solutions versus the length of the isolation period. *HB* Hopf bifurcation point, *sss* (locally asymptotically) stable steady state, *uss* unstable steady state, *sp* (locally asymptotically) stable periodic solution

homoclinic bifurcations. In Wu and Feng [17], the authors study this possibility for the *SIQR* model proposed in [8]. Using a simplification to the model, the existence of a homoclinic bifurcation in a three-parameter unfolding is established. We conduct a similar analysis for our expanded *SEIQR* model.

6.1 The simplified system

As mentioned before, $\nu \ll \theta_1, \theta_2, \zeta$ since $\frac{1}{\nu}$ denotes the average life expectancy and $\frac{1}{\theta_1}$, $\frac{1}{\theta_2}$, and $\frac{1}{\zeta}$ denote the average lengths of the latent, infectious, and isolated periods, respectively. Hence, we shall assume that $\nu = 0$ (i.e. our model has no death). Since we are looking for sophisticated dynamics, we expect to find most of them at the threshold $\mathcal{R}_0 = 1$. Recalling (5), we see that this is equivalent to setting $\theta_2 = 1$. Under these assumptions, our system becomes

$$\begin{aligned}
\frac{dz}{d\tau} &= p(1 - r - p) - z(\theta_1 + \zeta q),\\
\frac{dp}{d\tau} &= \theta_1 p + p(p - \zeta q),\\
\frac{dq}{d\tau} &= (q + 1)(p - \zeta q),\\
\frac{dr}{d\tau} &= r(p - \zeta q) + \zeta q.
\end{aligned} \tag{12}$$

Recalling (7) and (6), we see that these simplifications force our endemic equilibrium to coalesce with the DFE (i.e. $e_0 = (0, 0, 0, 0)$).

By the linear transformation

$$\begin{bmatrix} z \\ p \\ q \\ r \end{bmatrix} = \begin{bmatrix} 0 & \frac{1}{\theta_1} & 1 & 0 \\ 0 & 1 & -1 & 0 \\ 0 & \frac{1}{\zeta} & \frac{1}{1+\theta_1-\zeta} & 1 \\ 1 & 0 & \frac{\zeta}{(\theta_1+1)(\zeta-1-\theta_1)} & -1 \end{bmatrix} \begin{bmatrix} u \\ v \\ w \\ x \end{bmatrix}, \tag{13}$$

system (12) is transformed into

$$\begin{bmatrix} \dot{u} \\ \dot{v} \\ \dot{w} \\ \dot{x} \end{bmatrix} = \begin{bmatrix} 0 & 1 & 0 & 0 \\ 0 & 0 & 0 & 0 \\ 0 & 0 & -\theta_1 - 1 & 0 \\ 0 & 0 & 0 & -\zeta \end{bmatrix} \begin{bmatrix} u \\ v \\ w \\ x \end{bmatrix} + F(u, v, w, x), \tag{14}$$

where we suppress the expressions of the nonlinear terms for the sake of clarity. Note that the uv-plane is associated with a pair of zero eigenvalues, while the wx-plane corresponds to negative real eigenvalues. Through center manifold theory, we can limit our investigation of (12) to its restriction on the 2-dimensional center manifold of e_0 (see [16] for a detailed description).

The smooth center manifold $W^c(e_0)$ can be locally represented as:

$$\begin{aligned} W^c(e_0) = \{(u, v, w, x) \mid w = h_1(u, v), x = h_2(u, v), |u| < \delta, |v| < \delta, \\ h_i(0, 0) = Dh_i(0, 0) = 0 \text{ for } i = 1, 2\} \end{aligned} \tag{15}$$

for δ sufficiently small, where h_1, h_2 can be computed to any degree of accuracy using Taylor expansions. The center manifold theorem also concludes that the dynamics of (14) restricted to the center manifold is given by the first two equations in (14) with w replaced by $h_1(u, v)$ and x replaced by $h_2(u, v)$. Note that h_1, h_2 can not have constant or linear terms due to the last conditions of (15), so we can compute a second order approximation to $W^c(e_0)$ by setting

$$\begin{aligned} h_1(u, v) &= a_1u^2 + b_1uv + c_1v^2, \\ h_2(u, v) &= a_2u^2 + b_2uv + c_2v^2, \end{aligned} \tag{16}$$

and finding the appropriate constants. To do so, let us decouple (14) into the following form:

$$\begin{aligned} \begin{bmatrix} \dot{u} \\ \dot{v} \end{bmatrix} &= \begin{bmatrix} 0 & 1 \\ 0 & 0 \end{bmatrix} \begin{bmatrix} u \\ v \end{bmatrix} + f(u, v, w, x), \\ \begin{bmatrix} \dot{w} \\ \dot{x} \end{bmatrix} &= \begin{bmatrix} -\theta_1 - 1 & 0 \\ 0 & -\zeta \end{bmatrix} \begin{bmatrix} w \\ x \end{bmatrix} + g(u, v, w, x). \end{aligned} \tag{17}$$

Recalling that we hope to find $w = h_1(u, v),\ x = h_2(u, v)$, differentiation results in

$$\begin{bmatrix} \dot{w} \\ \dot{x} \end{bmatrix} = \begin{bmatrix} \frac{\partial h_1}{\partial u} & \frac{\partial h_1}{\partial v} \\ \frac{\partial h_2}{\partial u} & \frac{\partial h_2}{\partial v} \end{bmatrix} \begin{bmatrix} \dot{u} \\ \dot{v} \end{bmatrix}.$$

The center manifold is invariant under the dynamics of (17), so we must have that

$$\begin{aligned} &\begin{bmatrix} -\theta_1 - 1 & 0 \\ 0 & -\zeta \end{bmatrix} \begin{bmatrix} h_1(u, v) \\ h_2(u, v) \end{bmatrix} + g(u, v, h_1(u, v), h_2(u, v)) \\ &\quad = \begin{bmatrix} \frac{\partial h_1}{\partial u} & \frac{\partial h_1}{\partial v} \\ \frac{\partial h_2}{\partial u} & \frac{\partial h_2}{\partial v} \end{bmatrix} \left(\begin{bmatrix} 0 & 1 \\ 0 & 0 \end{bmatrix} \begin{bmatrix} u \\ v \end{bmatrix} + f(u, v, h_1(u, v), h_2(u, v)) \right). \end{aligned}$$

Substituting the expansions of h_1, h_2 given in (16), we can find the appropriate constants. Doing so and replacing w by $h_1(u, v)$ and x by $h_2(u, v)$, the system restricted to the center manifold is given by

$$\begin{aligned} \dot{u} &= v + \frac{\theta_1(\theta_1 + 1 + \zeta)}{\zeta(\theta_1 + 1)^2} uv + \frac{\theta_1 + 1 + \zeta}{\zeta(\theta_1 + 1)} v^2 + O(3), \\ \dot{v} &= \frac{-\theta_1}{\theta_1 + 1} uv - v^2 + O(3). \end{aligned} \tag{18}$$

We denote by $O(3)$ terms of order no less than three in u and v.

To further simplify (18), we shall use the normal form theorem. In essence, the method of normal forms allows one to determine a local coordinate system in which a particular dynamical system takes the "simplest" form. Of course, a suitable definition for "simplest" must be determined.

Utilizing a translation and linear transformation, we can assume that the linear part of any dynamical system is in Jordan canonical form and that the fixed point is at the origin. So the system has the form

$$\dot{\mathbf{x}} = J\mathbf{x} + F(\mathbf{x}) = J\mathbf{x} + F_2(\mathbf{x}) + F_3(\mathbf{x}) + \cdots + F_{m-1}(\mathbf{x}) + O(|\mathbf{x}|^m), \tag{19}$$

after expanding $F(\mathbf{x})$ in a Taylor series. Let H_k denote the linear space of vector-valued homogeneous polynomials of degree k. Define the map $L_J : H_k \to H_k$ by

$$L_J^{(k)}(\tilde{h}_k(\mathbf{x})) = -(D\tilde{h}_k(\mathbf{x})J\mathbf{x} - J\tilde{h}_k(\mathbf{x})).$$

Next, one can choose a complementary subspace in H_k for $L_J^{(k)}(H_k)$. Labeling this G_k, we have that $H_k = L_J^{(k)}(H_k) \oplus G_k$. We now recall the normal form theorem as stated in [16].

Theorem 3 (Normal form theorem) *By a sequence of analytic coordinate changes,* $\mathbf{x} \mapsto \mathbf{x} + \tilde{\mathbf{h}}_k(\mathbf{x})$, (19) *can be transformed into*

$$\dot{\mathbf{x}} = J\mathbf{x} + \mathbf{F_2^r}(\mathbf{x}) + \mathbf{F_3^r}(\mathbf{x}) + \cdots + \mathbf{F_{m-1}^r}(\mathbf{x}) + \mathbf{O}(|\mathbf{x}|^{\mathbf{m}}), \tag{20}$$

where $F_k^r(\mathbf{x}) \in \mathbf{G_k}$, *for* $2 \leq k \leq m-1$. *Equation* (20) *is said to be in normal form through order* $m-1$.

The definition of "simplest" that the theorem suggests is that a dynamical system is said to be in simplest form if all of the $O(|\mathbf{x}|^{\mathbf{k}})$ terms that remain are in a space complementary to $L_J^{(k)}(H_k)$ (i.e. are in G_k). Hence, simplicity is achieved by eliminating as much nonlinearity as possible.

Using normal form theory, we work to simplify the nonlinear terms as much as possible. In particular, we will find only the second order normal form for (18). By definition we have that

$$H_2 = \text{span}\left\{\begin{pmatrix}u^2\\0\end{pmatrix}, \begin{pmatrix}uv\\0\end{pmatrix}, \begin{pmatrix}v^2\\0\end{pmatrix}, \begin{pmatrix}0\\u^2\end{pmatrix}, \begin{pmatrix}0\\uv\end{pmatrix}, \begin{pmatrix}0\\v^2\end{pmatrix}\right\}.$$

Noticing that for system (18) the linear part is given by $J = \begin{bmatrix}1 & 0\\0 & 0\end{bmatrix}$, one can compute

$$L_J(H_2) = \text{span}\left\{\begin{pmatrix}-2uv\\0\end{pmatrix}, \begin{pmatrix}v^2\\0\end{pmatrix}, \begin{pmatrix}u^2\\-2uv\end{pmatrix}, \begin{pmatrix}uv\\-v^2\end{pmatrix}\right\},$$

and one choice of G_2 would be

$$G_2 = \text{span}\left\{\begin{pmatrix}0\\u^2\end{pmatrix}, \begin{pmatrix}0\\uv\end{pmatrix}\right\}.$$

Using the near-identity transformation

$$\begin{pmatrix}u\\v\end{pmatrix} \mapsto \begin{pmatrix}u\\v\end{pmatrix} + \begin{pmatrix}\left[\frac{-1}{2} - \frac{\theta_1+1+\zeta}{2\zeta(\theta_1+1)^2}\right]u^2 - \frac{\theta_1+1+\zeta}{\zeta(\theta_1+1)}uv\\ uv\end{pmatrix}, \tag{21}$$

i.e.

$$\tilde{h}_2(u,v) = \begin{pmatrix}\left[\frac{-1}{2} - \frac{\theta_1+1+\zeta}{2\zeta(\theta_1+1)^2}\right]u^2 - \frac{\theta_1+1+\zeta}{\zeta(\theta_1+1)}uv\\ uv\end{pmatrix},$$

we have that (18) can be transformed into

$$\begin{aligned}\dot{u} &= v + O(3),\\ \dot{v} &= \frac{-\theta_1}{\theta_1+1}uv + O(3).\end{aligned} \tag{22}$$

6.2 Unfolding analysis and bifurcations

In studying bifurcations of dynamical systems, one is interested in the effect of arbitrarily small perturbations to the system. For instance, "Can a small perturbation

destroy a certain bifurcation?" or "Can a small perturbation produce new qualitative behavior and hence a new bifurcation?" To deal with such questions, one can introduce small perturbations called *unfoldings* to a system. In special rare instances, one can then prove that an unfolding is *universal*, meaning that the family of systems created through varying the perturbation terms exhibits all possible qualitative behaviors near the bifurcation. Unfortunately, it can be shown that system (22) requires at least three unfolding parameters for a universal unfolding, making a complete bifurcation analysis extremely difficult. Fortunately, the goals of our unfolding are specific and hence a complete bifurcation analysis is unnecessary.

Our aim is to find an unfolding of system (22), that exhibits both homoclinic and Hopf bifurcations. While we have already proven Hopf bifurcation for the full system (3), it is desirable that the unfolding of the simplified system still demonstrates this feature.

Recall from Proposition 1 that the biologically feasible region for the original system is $B = \{(p, z, q, r) : z, p, q, r \geq 0 \text{ and } z + p + r \leq 1\}$. It follows from (13) that

$$u = \frac{-\theta_1(\zeta + 1 + \theta_1)}{\zeta(\theta_1 + 1)^2} z + \frac{\zeta - \theta_1 - \theta_1^2}{\zeta(\theta_1 + 1)^2} p + q + r,$$
$$v = \frac{\theta_1}{\theta_1 + 1} z + \frac{\theta_1}{\theta_1 + 1} p.$$

Thus, biological considerations require that $0 \leq v < 1$ after center manifold reduction. Also, recall that to compute the first order normal form, we used the near-identity transformation defined by (21). Noting that $v \mapsto v + uv$, we now have that $0 \leq v + uv < 1$. Considering this region and recalling that we are interested in finding bifurcations in a neighborhood of the fixed point $(0, 0)$, we must have that $v \geq 0$.

With this in mind, we propose the following unfolding of (22).

$$\begin{aligned} \dot{u} &= \sigma_1 u + v, \\ \dot{v} &= (\sigma_2 - \sigma_1)v + \alpha u^2 - \tfrac{\theta_1}{\theta_1+1} uv, \end{aligned} \tag{23}$$

where $\alpha \geq 0$ and all of $\sigma_1, \sigma_2, \alpha$ are small. When constructing unfoldings of a two-dimensional system, it is customary to add unfolding terms to the second equation only, without loss of generality. However, the equilibria of such perturbed systems would satisfy $v = 0$. Thus, any periodic orbits around an equilibrium would enter the biologically infeasible region of $v < 0$.

To facilitate analysis, we consider the case when α is a fixed positive constant and rescale by letting

$$u \to \frac{\alpha(\theta_1 + 1)^2}{\theta_1^2} u, \quad v \to \frac{\alpha^2(\theta_1 + 1)^3}{\theta_1^3} v, \quad t \to \frac{\theta_1}{\alpha(\theta_1 + 1)} t,$$
$$\sigma_1 \to \frac{\alpha(\theta_1 + 1)}{\theta_1} \mu_1, \quad \sigma_2 \to \frac{\alpha(\theta_1 + 1)}{\theta_1} \mu_2.$$

The resulting system is

$$\begin{aligned} \dot{u} &= \mu_1 u + v, \\ \dot{v} &= (\mu_2 - \mu_1)v + u^2 - uv, \end{aligned} \tag{24}$$

where μ_1, μ_2 are new parameters. System (24) has two equilibria $E_0 = (0, 0)$ and $E^* = (u^*, v^*)$, where

$$u^* = \frac{\mu_1(\mu_2 - \mu_1)}{\mu_1 + 1}, \qquad v^* = \frac{\mu_1^2(\mu_1 - \mu_2)}{\mu_1 + 1}.$$

To find a Hopf bifurcation, we consider the parameter region $\mu_2 \leq \mu_1$.

Theorem 4 *A supercritical Hopf bifurcation occurs for system* (24) *along the curve* $H = \left\{(\mu_1, \mu_2) : \mu_2 = -\mu_1^2, \mu_1 > 0\right\}$.

Proof The Jacobian of our system at E^* is

$$DF = \begin{bmatrix} \mu_1 & 1 \\ \frac{\mu_1(2+\mu_1)(\mu_2-\mu_1)}{\mu_1+1} & \frac{\mu_2-\mu_1}{\mu_1+1} \end{bmatrix}.$$

Noting that

$$\text{trace}(DF) = \frac{\mu_1^2 + \mu_2}{\mu_1 + 1} \quad \text{and} \quad \det(DF) = \mu_1(\mu_1 - \mu_2),$$

we consider the case when $\mu_2 = -\mu_1^2$. Here, we have that $\text{trace}(DF) = 0$ and $\det(DF) = \mu_1^2(\mu_1 + 1) > 0$, so the eigenvalues must be complex conjugates in a neighborhood of $\mu_2 = -\mu_1^2$. Thus, for each fixed μ_1, the eigenvalues cross the imaginary axis when μ_2 crosses $-\mu_1^2$. It is easy to check that this crossing is transversal and hence a Hopf bifurcation exists. Calculating the quantity defined as σ in [13] (§4.4, Rmk 1), we obtain $\sigma = \frac{-3\pi}{2\mu_1^3\sqrt{\mu_1+1}} < 0$. Thus the bifurcation is supercritical and results in a family of stable periodic orbits for $\mu_2 > -\mu_1^2$. This completes the proof.

Having confirmed that our unfolded system exhibits Hopf bifurcation, we proceed to the main goal of demonstrating the presence of homoclinic bifurcation.

Theorem 5 *A homoclinic bifurcation occurs for system* (24) *along the curve* $HC = \left\{(\mu_1, \mu_2) : \mu_2 = -\frac{6}{7}\mu_1^2 + O(\mu_1^3), \mu_1 > 0\right\}$.

Proof We follow closely the analysis of [17]. To greatly simplify the analysis, we begin by rescaling

$$u \to \epsilon^2 u, \quad v \to \epsilon^3 v, \quad \mu_1 \to \epsilon, \quad \mu_2 \to -\epsilon^2 \omega, \quad t \to \frac{t}{\epsilon}, \tag{25}$$

where ϵ and ω are new parameters. Under this rescaling, (24) becomes

$$\begin{aligned} \dot{u} &= u + v, \\ \dot{v} &= -v + u^2 - \epsilon(uv + \omega v), \end{aligned} \tag{26}$$

and the benefit of our rescaling becomes apparent. For $\epsilon = 0$, (26) is a Hamiltonian system with Hamiltonian given by

$$H(u, v) = \frac{v^2}{2} + uv - \frac{u^3}{3}. \tag{27}$$

Hence, (26) can be viewed as a perturbation to a Hamiltonian system. When $\epsilon = 0$, the trajectory corresponding to $H(u, v) = 0$ is a separatrix cycle, which we denote as $\Gamma_0 \cup \{0\}$. Explicitly, the separatrix cycle is

$$v_\pm(u) = -u \pm \frac{\sqrt{3}}{3} u\sqrt{3 + 2u}, \quad -\frac{3}{2} \le u \le 0. \tag{28}$$

Let $\gamma_0(t) = (u_0(t), v_0(t))$ be the solution on Γ_0, and let

$$\begin{aligned} \mathbf{f}(\gamma_0(t)) &= \begin{pmatrix} f_1(\gamma_0(t)) \\ f_1(\gamma_0(t)) \end{pmatrix} = \begin{pmatrix} u_0(t) + v_0(t) \\ -v_0(t) + u_0^2(t) \end{pmatrix}, \\ \mathbf{g}(\gamma_0(t), \omega) &= \begin{pmatrix} g_1(\gamma_0(t), \omega) \\ g_1(\gamma_0(t), \omega) \end{pmatrix} = \begin{pmatrix} 0 \\ -(\omega + u_0(t))v_0(t) \end{pmatrix}. \end{aligned} \tag{29}$$

We prove the existence of homoclinic bifurcations using Melnikov's method as described in [13]. The Melnikov function is defined as

$$M(\omega) = \int_{-\infty}^{\infty} \mathbf{f}(\gamma_0(t)) \wedge \mathbf{g}(\gamma_0(t), \omega)\, dt,$$

where $\mathbf{a} \wedge \mathbf{b} = a_1 b_2 - b_1 a_2$. Noticing that our expressions for $\mathbf{f}$ and $\mathbf{g}$ are the same as in [17], the resulting Melnikov function will also be the same. Hence, we have that $M(\omega) = \frac{6}{35}(6 - 7\omega)$. It follows that $M(\omega) = 0$ if and only if $\omega = 6/7$. Also, we note that $M_\omega(6/7) \neq 0$. Using a result in [13] (§4.9 Theorem 4), we can conclude that for all sufficiently small $\epsilon \neq 0$, there is a $\omega_\epsilon = 6/7 + O(\epsilon)$ such that (26) has a homoclinic orbit Γ_ϵ when $\omega = \omega_\epsilon$. Recalling that $\mu_1 = \epsilon$ and $\mu_2 = -\epsilon^2\omega$, we see that the homoclinic bifurcation for (24) occurs at $\mu_2 = -\frac{6}{7}\mu_1^2 + O(\mu_1^3)$. This completes the proof.

7 Comparison to historical data

7.1 Scarlet fever Data, England and Wales, 1897–1978

Using the historical data of Anderson and May [2, Tables 3.1, 3.3, and 6.1], we can examine the range of isolation periods which result in sustained oscillations. To apply the data to our model, we follow closely the approach of [8]. The reasoning for doing so is to exhibit only those changes that result from the inclusion of the latent class.

Since the results of Sect. 4 are formulated in a scaled time, knowledge of σ, the per capita infection rate, is needed in order to return to real time. Unfortunately, the infection rate is one of the most difficult rates to estimate from real data. To do so implicitly, we recall the expression for $\mathcal{R}_0$ given in (5). As mentioned before, we expect that $\nu \ll \theta_1, \theta_2, \zeta$ for biologically reasonable parameters and it follows that $\mathcal{R}_0 \approx 1/\theta_2$. Hence, when $\mathcal{R}_0$ and γ_2 are determined, a value for σ is easily obtained using the relation $\sigma = \gamma_2/\theta_2 = \gamma_2\mathcal{R}_0$.

Feng and Thieme [8] are able to obtain bounds for $\mathcal{R}_0$ that depend only on the average age at infection (or mean sojourn time in the susceptible class), average life expectancy, and the mean interepidemic period. Using data reported in [1,2], an average age at infection of 12 years, an average life expectancy of 65 years, and a mean interepidemic period of 4.4 years are assumed. As a result, the bounds for $\mathcal{R}_0$ are found to be $6.4 < \mathcal{R}_0 < 7.7$. Assuming that the sum of latent and effective infectious period is 3 days, a window for the length of isolation periods that result in sustained oscillations is found. For the lower estimate $\mathcal{R}_0 = 6.4$, isolation periods, D_Q, such that

$$22.8 \text{ days} < D_Q < 1.83 \text{ years} \tag{30}$$

result in an unstable endemic equilibrium. The window

$$26.7 \text{ days} < D_Q < 1.22 \text{ years} \tag{31}$$

is found when $\mathcal{R}_0 = 7.7$ (see [8] for details).

Anderson and May [2, Table 3.1] report a latent period lasting 1–2 days for scarlet fever. They also report an incubation period lasting 2–3 days and an infectious period that lasts 14–21 days. Here, the term *incubation period* refers to the time period between initial infection and the appearance of symptoms, whereas the latent period is the time period in which an individual is infected but not infectious. In some of the literature the terms are used interchangeably, but here we adopt the convention of Anderson and May. At the onset of symptoms, the most apparent being the scarlet-colored rash from which the disease gets its name, children are usually isolated (i.e. sick children stay at home). Thus, in terms of our model we assume an effective infectious period of only 1–2 days which corresponds to the period in which an individual is infectious but is yet to develop the symptoms that trigger isolation. We would then expect an isolation period of 13–20 days as most children are kept at home until symptoms cease.

Table 2 Bounds for isolation periods which result in sustained oscillations for the lower estimate $\mathcal{R}_0 = 6.4$

Latent period (days)	Average length of effective infectious period							
	1.00 days		1.33 days		1.66 days		2.00 days	
	Min (days)	Max (years)	Min (days)	Max (years)	Min (days)	Max (years)	Min (days)	Max (years)
1.00	12.0	2.23	14.0	2.22	16.2	2.20	18.5	2.17
1.33	14.0	2.22	15.9	2.23	18.0	2.22	20.1	2.21
1.66	16.2	2.20	18.0	2.22	19.9	2.23	22.0	2.22
2.00	18.5	2.17	20.1	2.21	22.0	2.22	23.9	2.23

Table 3 Bounds for isolation periods which result in sustained oscillations for the upper estimate $\mathcal{R}_0 = 7.7$

Latent period (days)	Average length of effective infectious period							
	1.00 days		1.33 days		1.66 days		2.00 days	
	Min (days)	Max (years)	Min (days)	Max (years)	Min (days)	Max (years)	Min (days)	Max (years)
1.00	13.8	1.52	16.2	1.52	18.7	1.50	21.4	1.49
1.33	16.2	1.52	18.4	1.52	20.8	1.52	23.3	1.51
1.66	18.7	1.50	20.8	1.52	23.0	1.52	25.4	1.52
2.00	21.4	1.49	23.3	1.51	25.4	1.52	27.7	1.52

To examine the model which includes the latent class, we use the bounds for $\mathcal{R}_0$ established in [8]. Since the model of [8] combines the latent and effective infectious periods, we are now forced to make additional assumptions on the respective lengths of the latent and effective infectious periods. For an efficient comparison to the previous work, we compute the window for several reasonable combinations of parameters. The results are summarized in Tables 2 and 3. Assuming that the sum of the latent and effective infectious periods was 3 days, the lower thresholds found in [8] for both the lower and upper estimate of $\mathcal{R}_0$ are larger than the expected 13–20 days. When explicitly including the latent class in the model, the situation improves. We see that the minimum length of the isolation period necessary for sustained oscillations is in general smaller and is often within the realistic range suggested by [2].

The periods of the periodic solutions which result from the Hopf bifurcation are dependent on the length of the isolation period. The observed lengths of interepidemic periods reported by Anderson and May [2, Table 6.1] are between 3 and 6 years. Assuming that the sum of the latent and effective infectious periods is 3 days, these lengths are feasible for the model without a latent class when the isolation period is between 27 and 57 days [8]. Using Auto, we examine several combinations of lengths for latent and effective infectious periods whose sum is 3 days. For all of the combinations considered, an interepidemic period of 3 years corresponds to an isolation period near 20 days. An interepidemic period of 6 years corresponds to isolation

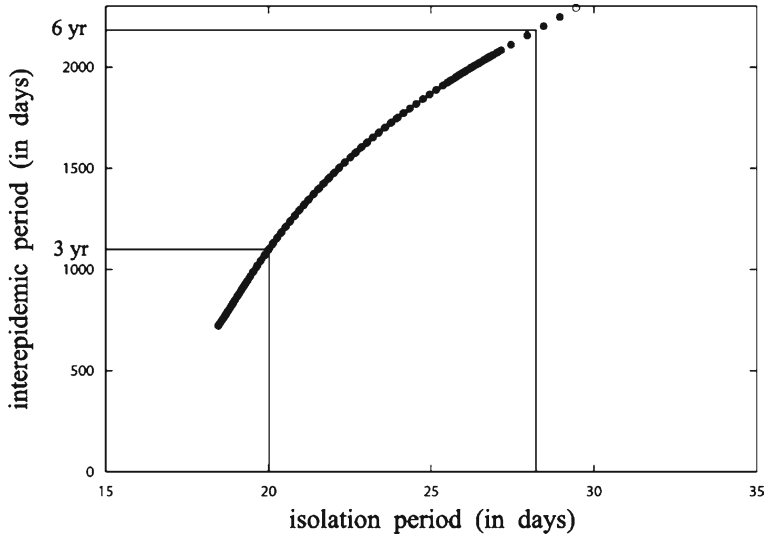

Fig. 4 An Auto plot of the periods of the periodic solutions versus the length of the isolation period when $\mathcal{R}_0 = 6.4$, $1/\gamma_1 = 1.5$, and $1/\gamma_2 = 1.5$

periods between 28 and 30 days. Figure 4 displays the results of the simulation when both the latent and effective infectious periods are assumed to be 1.5 days.

7.2 Other childhood diseases

While scarlet fever makes a compelling case for isolation as a factor of sustained oscillations in childhood diseases, the epidemiological uniqueness of the disease must be noted. The infectious period of scarlet fever (14–21 days) is very long compared to the incubation period (2–3 days) [2]. This allows for lengthy, and therefore highly effective isolation periods. Noting the estimates from [2] summarized in Table 4, we see that this is not a common attribute.

To examine the role that isolation may play in these diseases, we use realistic parameters for each disease and calculate the window of isolation periods that will

Table 4 Estimates of $\mathcal{R}_0$ along with incubation, latent, and infectious periods (in days) for common childhood diseases from Anderson and May [2]

Disease	Latent period	Incubation period	Infectious period	$\mathcal{R}_0$
Measles	6–9	8–13	6–7	12–13[a]
Mumps	12–18	12–26	4–8	10–12[a]
Rubella	7–14	14–21	11–12	9–10[a]
Varicella	8–12	13–17	10–11	9–10[a]

[a] Reported ranges for $\mathcal{R}_0$ obtained by averaging several estimates in [2]

Table 5 Parameters used along with the resulting bounds for isolation periods which result in sustained oscillations

Disease	$\frac{1}{\gamma_1}$	$\frac{1}{\gamma_2}$	$\mathcal{R}_0$	Feasible isolation	Min (days)	Max (days)
Measles	7.5	3	12.5	3–4	116	198
Mumps	15	4	11	0–4	195	245
Rubella	10.5	7	9.5	4–5	146	359
Varicella	10	5	9.5	5–6	127	352

result in sustained oscillations. Using the historical data, we also have estimates for feasible lengths of isolation. The results are summarized in Table 5. For each disease, the necessary length of isolation vastly exceeds those that are consistent with historical data. The evidence suggests that isolation has little or no impact on the periodic outbreaks of these diseases.

To further understand the length of isolation that is necessary to generate sustained oscillations, we reconsider the expression for the first Hopf bifurcation:

$$\zeta_0(\nu) = \frac{\theta_1\theta_2^2(1-\theta_2)(\theta_1+\theta_2)}{\theta_2^2(\theta_1+1)+\theta_1\theta_2+\theta_1^2} + O(\nu^{1/2}).$$

We denote by D_L, D_I, D_Q the average lengths of latent, infectious, and isolation periods, respectively (i.e. $D_L = \frac{1}{\gamma_1} = \frac{1}{\sigma\theta_1}, D_I = \frac{1}{\gamma_2} = \frac{1}{\sigma\theta_2}, D_Q = \frac{1}{\xi} = \frac{1}{\sigma\zeta}$). Recalling that sustained oscillations occur for $\zeta_1 < \zeta < \zeta_0$, which is equivalent to $\frac{1}{\sigma\zeta_0} < D_Q < \frac{1}{\sigma\zeta_1}$, we see that ζ_0 corresponds to the lower threshold for isolation. Using that $\mathcal{R}_0 \approx \frac{1}{\theta_2} = \sigma D_I$ and the above expressions for D_L, D_I, and D_Q we can obtain that the approximate minimum duration of isolation necessary for periodic behavior is given by

$$D_Q = \frac{\mathcal{R}_0^2}{\mathcal{R}_0-1}D_I + \frac{\mathcal{R}_0(D_L\mathcal{R}_0+D_I)}{(D_L+D_I)(\mathcal{R}_0-1)}D_L. \tag{32}$$

Considering only the simplified case where $D_L = 0$ and thinking in terms of a highly infectious disease with large $\mathcal{R}_0$, (32) yields

$$D_Q = \frac{\mathcal{R}_0^2}{\mathcal{R}_0-1}D_I \approx (\mathcal{R}_0+1)D_I. \tag{33}$$

In order to have sustained oscillations for a highly infectious disease, an isolation period that exceeds the infectious period by a factor of at least $\mathcal{R}_0 + 1$ is required. However, it appears that vaccination could play a role in relaxing this constraint. In the scenario of vaccination at birth conferring lifelong immunity, the basic reproductive number would be reduced to $(1-c)\mathcal{R}_0$, where c denotes the proportion of individuals vaccinated at birth. Provided that vaccination is not widespread/effective enough to

drive the reproductive number near 1, we might expect a lower threshold for necessary isolation.

7.3 Vaccination

In order to rigorously study the impact of vaccination, we incorporate vaccination into our original *SEIQR* system, (1). The resulting system is given by

$$\begin{aligned}
\frac{d}{dt}S &= (1-c)\Lambda - \mu S - \sigma S\frac{I}{A},\\
\frac{d}{dt}E &= -(\mu+\gamma_1)E + \sigma S\frac{I}{A},\\
\frac{d}{dt}I &= -(\mu+\gamma_2)I + \gamma_1 E,\\
\frac{d}{dt}Q &= -(\mu+\xi)Q + \gamma_2 I,\\
\frac{d}{dt}R &= -\mu R + \xi Q + c\Lambda,
\end{aligned} \tag{34}$$

where c denotes the proportion of individuals vaccinated at birth. Following the same simplifications and rescalings as in Sect. 2 (i.e. $N = \frac{\Lambda}{\mu}$, rescaling time by σ, etc.), the reduced system is expressed by

$$\begin{aligned}
\frac{dz}{d\tau} &= z[-\nu-\theta_1+\theta_2 p-(\nu+\zeta)q] + p(1-p-r-z),\\
\frac{dp}{d\tau} &= p[-\nu-\theta_2+\theta_2 p-(\nu+\zeta)q] + \theta_1 z,\\
\frac{dq}{d\tau} &= (1+q)[\theta_2 p-(\nu+\zeta)q],\\
\frac{dr}{d\tau} &= r[-\nu+\theta_2 p-(\nu+\zeta)q] + \zeta q + c(1+q)\nu.
\end{aligned} \tag{35}$$

All of the analysis used in Sect. 4 to locate the Hopf bifurcation for (3) can be applied to (35). In doing so, we find the threshold for ζ corresponding to the lower bound of the isolation window is given by

$$\zeta_0^V(\nu) = \frac{\theta_1\theta_2^2(\theta_1+\theta_2)(1-c-\theta_2)}{(1-c)(\theta_1^2+\theta_1\theta_2+\theta_2^2)+\theta_1\theta_2^2} + O(\nu^{1/2}). \tag{36}$$

Investigating the role of vaccination, we find that

$$\frac{\partial\zeta_0^V}{\partial c} = \frac{-\theta_1\theta_2^3(\theta_1+\theta_2)^3}{[(1-c)(\theta_1^2+\theta_1\theta_2+\theta_2^2)+\theta_1\theta_2^2]^2} + O(\nu^{1/2}) < 0,$$

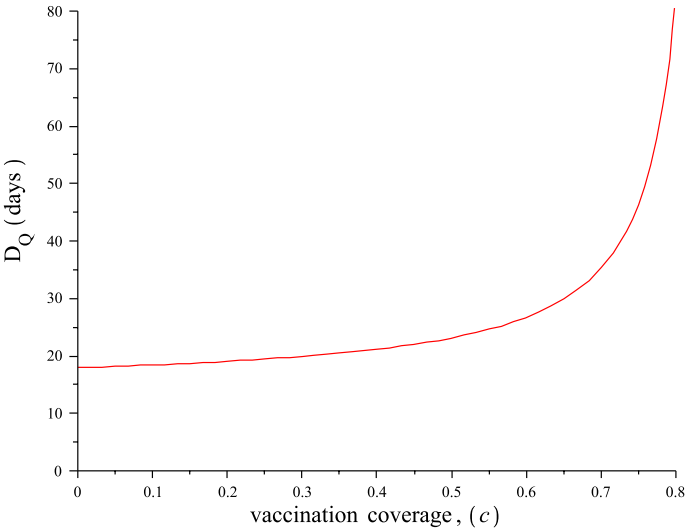

Fig. 5 Minimum isolation period necessary for periodic behavior as a function of vaccine coverage for scarlet fever. Parameters: $D_L = D_I = 1.5$ days, $\mathcal{R}_0 = 6.4$

provided that ν is small enough. With ζ_0^V being a decreasing function of c, we have that any increase in vaccination will correspondingly increase the minimum isolation period necessary to produce sustained oscillations. An example of this behavior is depicted in Fig. 5 for the case of scarlet fever. Since $\mathcal{R}_0$ is assumed to be 6.4, we expect to see a singularity for $c = \frac{\mathcal{R}_0 - 1}{\mathcal{R}_0} \approx 0.84$ as this corresponds to the condition that $(1 - c)\mathcal{R}_0 = 1$. At this threshold, the endemic equilibrium coalesces with the disease free equilibrium and is globally asymptotically stable. Thus, periodic behavior can not occur regardless of isolation.

Contrary to the intuition gained from (33), vaccination, at any level, has a stabilizing effect on the endemic equilibrium. Therefore, in the presence of vaccination, isolation becomes even less plausible a factor for the sustained oscillations of childhood diseases.

8 Discussion

Feng and Thieme [8] showed that the inclusion of an isolated class in the standard SIR model for childhood diseases can give rise to sustained oscillations. Their model neglects the latency period, which can often be as long or longer than the infectious period for childhood diseases [2].

In this work, we extend the model of [8] to include the latent class. The basic reproductive number and endemic equilibrium are computed. We then move on to prove the existence of two Hopf bifurcations. With the expressions of the Hopf bifurcations in hand, we gain knowledge about the regions of parameter space that give rise to sustained oscillations (see Fig. 1). We find that the inclusion of the latent class can destroy the sustained oscillations provided that the latent period is long enough.

Numerical work indicates a possibility for homoclinic orbits. To examine this further, we consider arbitrarily small perturbations to a simplified version of our model. Using analysis similar to that of [17], we are able to prove the existence of both Hopf and homoclinic bifurcation in the perturbed model. We conclude by comparing our model to historical data for childhood diseases in England and Wales obtained from [2]. Our model agrees with the data more closely than the model without the latent class. In the case of scarlet fever, our model exhibits sustained oscillations for isolation periods within the realistic range. For other childhood diseases, which are less conducive to effective isolation, the necessary lengths of isolation to produce periodic behavior far exceed realistic values.

This work demonstrates the destabilizing effect that autonomous, deterministic factors alone can have on the endemic equilibrium of a childhood disease model. For scarlet fever, these factors are able to produce sustained oscillations for feasible lengths of the isolation period. This observation is not contrary to the belief that the periodic behavior of childhood diseases is connected to forces such as seasonal transmissibility, stochasticity, and school year schedule. In fact, for various other childhood diseases, our model suggests that isolation is unlikely to be a factor in sustained oscillations. However, the work does give insight into the types of diseases that are most likely to be influenced by these autonomous, deterministic factors.

References

1. Anderson RM, May RM (1982) Directly transmitted infectious diseases: control by vaccination. Science 215:1053–1060
2. Anderson RM, May RM (1992) Infectious diseases of humans: dynamics and control. Oxford University Press, New York
3. Bernoulli D (1976) Essai d'une nouvelle analyse de la mortalité causée par la petite vérole. Mem Math Phy Acad Roy Sci Paris (1766). English translation entitled 'An attempt at a new analysis of the mortality caused by smallpox and of the advantages of inoculation to prevent it' In: Bradley L (ed) Smallpox Inoculation: An Eighteenth Century Mathematical Controversy, Adult Education Department, Nottingham, 1971, p 21
4. Diekmann O, Heesterbeek J (2000) Mathematical epidemiology of infectious diseases: Model building, analysis and interpretation. Wiley, Chichester
5. Doedel E (1981) Auto: a program for the automatic bifurcation analysis of autonomous systems. Congr Numer 30:265–284
6. Emerson H (1937) Measles and whooping cough. Am J Public Health 27:1–153
7. Feng Z (1994) A mathematical model for the dynamics of childhood diseases under the impact of isolation. Ph.D. thesis, Arizona State University
8. Feng Z, Thieme HR (1995) Recurrent outbreaks of childhood diseases revisited: the impact of isolation. Math Biosci 128:93–130
9. Gao LQ, Mena-Lorca J, Hethcote HW (1995) Four *SEI* endemic models with periodicity and separatrices. Math Biosci 128:157–184
10. Greenhalgh D (1990) Deterministic models for common childhood diseases. Int J Syst Sci 21:1–20
11. Kato T (1984) Perturbation theory for linear operators. Springer, Berlin
12. London WP, Yorke JA (1973) Recurrent outbreaks of measles, chickenpox and mumps. Am J Epidemiol 98:453–468
13. Perko L (1996) Differential equations and dynamical systems, 2nd edn. Springer, New York
14. Thieme HR (1992) Epidemic and demographic interaction in the spread of potentially fatal diseases in growing populations. Math Biosci 111:99–130
15. Thieme HR (1993) Persistence under relaxed point-dissipativity (with applications to an endemic model). SIAM J Math Anal 24:407–435

16. Wiggins S (2003) Introduction to applied nonlinear dynamical systems and chaos, 2nd edn. Springer, New York
17. Wu LI, Feng Z (2000) Homoclinic bifurcation in an *SIQR* model for childhood diseases. J Differ Equ 168:150–167
18. Zhou J, Hethcote HW (1994) Population size dependent incidence in models for diseases without immunity. J Math Biol 32:809–834